technologies

MDPI

*Review*

# Artificial Tissue Models for Microneedle Testing and Analysis

**Elham Lori Zoudani [1,2] and Navid Kashaninejad [1,2,*]**

[1] School of Engineering and Built Environment, Griffith University, 170 Kessels Road, Nathan, Brisbane, QLD 4111, Australia; elham.lorizoudani@griffithuni.edu.au
[2] Queensland Quantum and Advanced Technologies Research Institute, Griffith University, 170 Kessels Road, Nathan, Brisbane, QLD 4111, Australia
* Correspondence: n.kashaninejad@griffith.edu.au

**Abstract**

The role of microneedles (MNs) in enhancing tissue permeability has long been established. Their capacity to serve as drug-delivery vehicles or biosensing platforms makes them ideal candidates for applications in which tissue serves as the primary pathway. Such potential can only be thoroughly validated through tissue-dependent tests. Although MNs are not limited to human tissues, humans remain the most relevant target group. This highlights the need to develop platforms that closely replicate the structure of human tissue for the intended applications. To date, many studies have addressed the limited availability of human samples, constrained by ethical concerns and other challenges, by using artificial, human-like tissue mimics. These models have been widely used to evaluate various aspects of MN performance, including penetrability, drug delivery, and biosensing. Despite limitations, artificial tissues provide a practical assessment tool in MN development. This review offers new insights into the role of synthetic tissue models in evaluating MN functionality. It discusses the underlying rationale for their use, highlights their flexibility and potential in MN application studies, addresses their limitations, and presents their future perspective. Finally, it highlights the need for standardized, scalable artificial tissue platforms to support the translational and commercial advancement of MN technologies.

**Keywords:** skin phantom; tissue-mimetic biomaterials; transdermal drug delivery; microneedles; biosensing

## 1. Introduction

In device development, a well-defined characterization platform is a prerequisite for achieving an efficient and optimized final product. MN development is no exception. Given their intended applications, it is essential to conduct systematic evaluations of their performance in order to achieve the most effective MN design [1]. Since MNs primarily interact with biological tissue, an appropriate tissue model for initial evaluation is critical. Humans represent the primary target group for these devices, making human skin the ideal model. However, ethical constraints and the limited availability of fresh human tissue make comprehensive testing across different tissue types nearly impossible. Moreover, recent studies have highlighted the potential of MNs not only for transdermal use but also for applications involving internal tissues [2,3], further underscoring the impracticality of obtaining all relevant biological samples. This creates a pressing need for models that closely replicate the structural and mechanical properties of real tissues. Thus, alongside optimizing MN design and materials, it is equally essential to ensure that the tissue models employed are as physiologically relevant as possible.



Academic Editor: Dennis Douroumis

Received: 29 December 2025
Revised: 23 January 2026
Accepted: 2 February 2026
Published: 8 February 2026

In recent years, artificial tissues, particularly polymer-based models such as agarose gel, polydimethylsiloxane (PDMS), and Parafilm, have provided new opportunities to characterize MN systems and analyze diverse aspects of their performance [4,5]. Their significance has become increasingly evident. Without such models, the ability to systematically evaluate MN performance would have been severely limited, hindering progress in biomedical applications. Artificial tissues have been particularly valuable for assessing mechanical performance, such as insertion and extraction behavior. For example, agarose gel has been widely used to investigate MN penetration capabilities, and it has also been employed in drug delivery studies, where release and diffusion processes can be assessed in vitro [6–8]. Similarly, artificial tissues have been used in biosensing applications, further demonstrating their versatility and importance. Three-dimensional microfluidic culture systems have also been widely employed as engineered tissue analogues, as they enable controlled investigation of oxygen and nutrient transport, shear stress, and cellular organisation under well-defined geometric and perfusion conditions [9].

This review explores the diverse applications of artificial tissues in MN research, with a particular emphasis on their role as platforms for characterization and performance evaluation rather than as biological substitutes alone. While numerous studies have reported individual tissue-mimicking models for specific MN applications, a consolidated perspective linking model selection to the particular performance metrics being evaluated remains limited. Here, artificial tissue models are examined across mechanical testing, therapeutic delivery, and biosensing applications, highlighting how different material choices and platform designs influence experimental outcomes. By organising the literature around the functional role of artificial tissues in MN development, this review aims to support more informed selection of tissue models and to clarify their advantages and limitations at different stages of MN research. The review concludes with a discussion of future perspectives and directions for research in this area.

## 2. Why Artificial Tissues?

The rationale for employing artificial tissue models is to establish reliable, accessible platforms for MN testing and evaluation. The use of real tissue samples often entails significant challenges. Ethical approval and regulatory requirements for animal models create delays, which, in turn, affect research timelines and resource allocation [10]. In addition, animal testing requires strict storage and maintenance conditions, with high associated costs that pose a significant obstacle, particularly during the early stages of MN development.

Artificial synthetic tissue models, by contrast, are readily available and offer a high degree of flexibility. Their properties can be customized to mimic the mechanical and structural characteristics of target tissues, a level of control that is not achievable with in vivo or ex vivo samples. For instance, animal skin, e.g., porcine skin, commonly used as one of the closest analogues to human skin, still exhibits variability in properties depending on factors such as storage conditions, animal age, and anatomical origin. These variations may not align with the specific tissue type for which MNs are designed, limiting the reliability of results.

Artificial models are scalable and suitable for industrial and commercial applications. Their ease of preparation and tunability make them highly practical for multiple testing purposes. Furthermore, they enable the modeling of extreme physiological conditions that would be unsafe or impractical to replicate in vivo. In drug delivery applications, these models provide a valuable platform for early-stage formulation optimization, including dosage determination, prior to extensive in vivo studies.

## 3. Applications of Artificial Tissue Models

As tools for MN testing and characterization, artificial tissue-mimetic models have been employed for various evaluation purposes. These models provide a means to study microneedle–tissue interactions across a wide range of applications. Their ability to replicate the mechanical and diffusional characteristics of real tissue samples makes them particularly valuable for assessing MN performance in therapeutic and biosensing fields. In the following subsections, selected studies in this area are presented.

### *3.1. MN-Tissue Mechanical Interaction Analysis*

In MN applications, tissue serves as the primary pathway, and all factors influencing MN–tissue interactions directly affect device performance. These include insertion force, penetration depth, and extraction force in the case of non-dissolvable microneedles. To facilitate systematic experimentation and iterative optimization, a variety of artificial skin models have been developed.

Parafilm®M, composed of hydrocarbon wax and polyolefin, is commonly employed as a membrane model to simulate layered tissue structures in MN penetration studies. For instance, eight layers of Parafilm were used in vitro to mimic the thickness of human skin, with each layer averaging 126 μm in thickness. The insertion capability of microneedle patches with different formulations was quantified by measuring the number of layers penetrated [11]. In another study, an MN insertion setup was used to analyze MN penetration depth, as shown in Figure 1A. As in the previous approach, eight layers of Parafilm®M were stacked together as the tissue model. Penetration depth was evaluated by calculating the percentage of holes created by the MNs at each layer of Parafilm [12].

Agarose gel, a hydrogel widely used in biomedical applications [13], has also demonstrated utility as a tissue-mimetic model due to its viscoelastic properties, which resemble those of hydrated biological tissues. In MN studies, agarose gels have been employed to measure MN insertion and extraction forces, as well as to assess MN tissue adhesiveness through quantification of extraction behavior [6,14]. These characteristics make agarose gel a valuable model for studying MN performance in hydrated tissue environments [14].

In another study, Makvandi et al. developed a composite tissue model composed of a silicone layer and a gel layer, designed to mimic the stratum corneum and the hydrated viable epidermis/dermis, respectively [15]. The tissue structure is shown in Figure 1B. This artificial model was proposed as an alternative to in vivo or ex vivo tissue samples for testing MN penetration. The silicone layer, incorporated to replicate the stratum corneum, was used to evaluate the insertion performance of hydrogel microneedle arrays across subcutaneous tissue layers. Penetration tests were conducted using three substrates: porcine skin, agarose gel, and the engineered tissue model. The findings showed that, with respect to MN penetrability, the tissue model yielded results more comparable to those from porcine skin than agarose gel. The channel widths formed by MN insertion were ≈300 μm in ex vivo porcine skin and ≈280 μm in the tissue model, both significantly wider than those generated in agarose gel (>10 μm). Figure 1C shows the MNs' penetration into the tissue model.

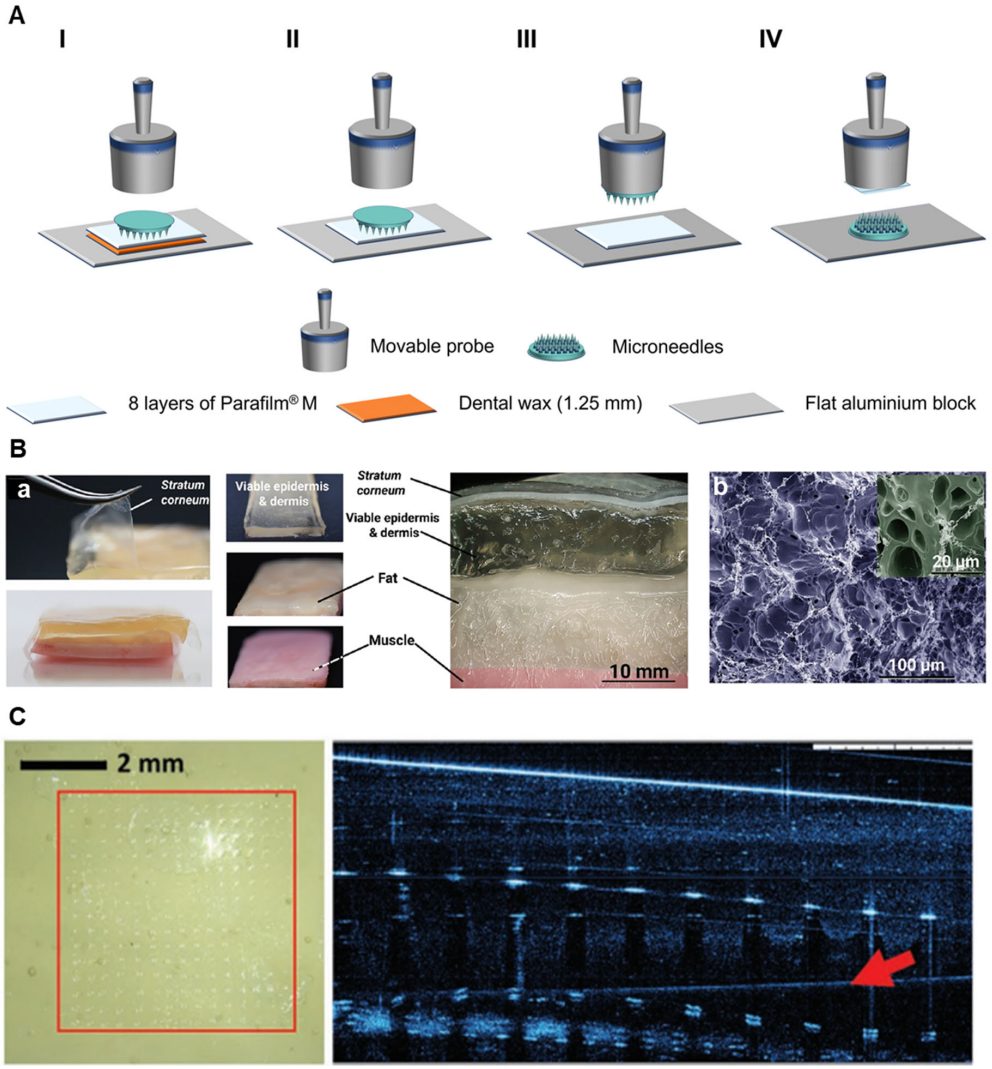


**Figure 1.** Representative artificial tissue models, experimental configurations, and imaging methods used to study MN–tissue mechanical interactions. (**A**) Schematic configurations of four different MN penetration test setups. (**I**) MNs (needles down) inserted into stacked Parafilm®M layers supported by dental wax. (**II**) MNs (needles down) inserted into unsupported stacked Parafilm®M layers. (**III**) MNs (needles down) mounted on a movable probe, with Parafilm®M layers fixed to the stage. (**IV**) MNs (needles up) fixed on the stage, with Parafilm®M layers mounted on the probe. Reproduced from [12] under the terms of the Creative Commons Attribution 3.0 License (CC BY 3.0). (**B**) (**a**) Photograph of the synthesized multi-layered tissue model, with each layer representing a specific component of human skin; (**b**) Scanning Electron Microscopy (SEM) images of the gel layer within the tissue model. (**C**) Optical microscopy (**left**) and optical coherence tomography (OCT, (**right**)) images of MN penetration into the tissue model (red arrow indicates the tissue surface). Adapted from [15] under the terms of the Creative Commons CC BY license.

## Non-Transdermal Tissue Phantoms for Mechanical Interaction Analysis

Although the majority of artificial tissue models for MN mechanical testing have been developed for transdermal applications, there is increasing interest in extending MN technologies to non-transdermal targets, such as ocular and other internal tissues. Compared with skin, these tissues exhibit distinct mechanical and interfacial characteristics, including higher hydration levels, lower stiffness, curved geometries, and lubricated surfaces, which necessitate the development of purpose-designed artificial phantoms rather than direct reuse of skin-mimicking models.

As evidence of the applicability of artificial tissue phantoms for non-transdermal applications, the tissue adhesiveness of a hydrogel MN array with a self-adhesive design was evaluated using a sclera-mimicking phantom [16]. It was prepared from polycaprolactone in 5% (*w*/*v*) chloroform and integrated with a vitreous humor-mimicking gel (PVA mixed with 2.5% (*w*/*v*) gelatin in water) and an ex vivo rabbit eye model. The results showed comparable results for these cases with no significant difference in adhesion forces between the two tissue models, with values of approximately 2.0 N for the phantom and 2.2 N for the ex vivo tissue. A similar trend was also observed for the measured penetration forces.

Beyond ocular systems, recent reviews of 3D-printed polymeric microneedle arrays highlight rapid growth in non-transdermal MN applications targeting the oral cavity, gastrointestinal tract, central nervous system, cardiovascular tissues, and reproductive organs [17]. However, these studies predominantly focus on the feasibility of MN fabrication and delivery, and most evaluations rely on ex vivo tissues, animal models, or highly simplified gels rather than standardized artificial tissue surrogates. This contrast underscores a current gap between the expanding scope of non-transdermal MN technologies and the availability of validated artificial tissue models for their mechanical characterization, indicating a clear opportunity to develop application-specific non-skin phantoms.

### *3.2. Drug Delivery and Therapeutic Evaluation*

The use of artificial tissue models has created new opportunities for MN testing in therapeutic applications such as drug delivery. These tissue-mimicking platforms enable comprehensive analysis of various aspects of the drug release process. For instance, the transparency of agarose gel makes it a suitable candidate for visualizing drug diffusion pathways. Ramalheiro et al. demonstrated the release profile of fluorescently labeled theranomycin-loaded cubosome-like particles using agarose gel as a tissue model [18]. The particles were incorporated into dissolving microneedles, which fully dissolved in 3% agarose gel within one minute, releasing their cargo into the gel matrix.

Biological variability in real tissues often masks the effects of experimental parameters, thereby directly affecting the reliability and reproducibility of results. Since these artificial tissues are free of biological interference, the analysis can focus solely on the intended aspects of the platform without concern for undesired or uncontrolled biological factors. This is particularly important in cases such as protein or peptide transdermal delivery, where the use of real biological tissues can complicate analysis due to protein interference. As proven by Anjani et al. artificial models such as Parafilm®M and Strat-M® can be as reliable alternatives to dermatomed porcine skin [19]. Strat-M®, engineered to mimic human skin, consists of multiple layers: a lipid-based outer layer representing the stratum corneum; a porous polyether sulfone middle layer simulating the dermis; and a polyolefin non-fabric support layer mimicking the subcutaneous tissue. Figure 2A,B schematically illustrate the structure of these tissue models. These artificial models were employed to evaluate dissolving microneedle patches for transdermal delivery of proteins including ovalbumin (OVA), bovine serum albumin (BSA), and amniotic mesenchymal stem cell metabolite products (AMSC-MP). Optical microscope images of the top surface and SEM images of the backside of OVA-loaded dissolving microneedles after penetration into Parafilm®M and Strat-M® are shown in Figure 2C. Based on cumulative permeation studies of the three protein models across Parafilm®M, Strat-M®, and dermatomed porcine skin, permeation levels varied across both tissue types and proteins. The cumulative permeation of OVA-loaded dissolving microarray patches across dermatomed porcine skin, Parafilm®M, and Strat-M® was 14.21%, 12.31%, and 17.27%, respectively, with no significant differences after normalization ($p > 0.05$). For BSA, 24 h permeation was 54.45%, 26.59%, and 11.14%, respectively, with porcine skin showing a significantly higher (4.88-fold) permeation than Strat-M® ($p < 0.05$),

likely due to interference from endogenous skin proteins. Similarly, AMSC-MP permeation reached 110.05%, 94.59%, and 33.41%, respectively, with Parafilm®M showing a 2.83-fold higher permeation than Strat-M® ($p < 0.05$) and no significant difference from porcine skin ($p > 0.05$). Correlation analysis over 24 h revealed protein-dependent agreement between Parafilm®M and Strat-M®, with strong and moderate correlations for OVA and BSA, respectively, and a very strong correlation for AMSC-MP (r = 0.90–0.99). In contrast, correlations with dermatomed porcine skin were poor due to protein interference, indicating that Parafilm®M and Strat-M® provide more reliable and reproducible permeation data than neonatal porcine skin.

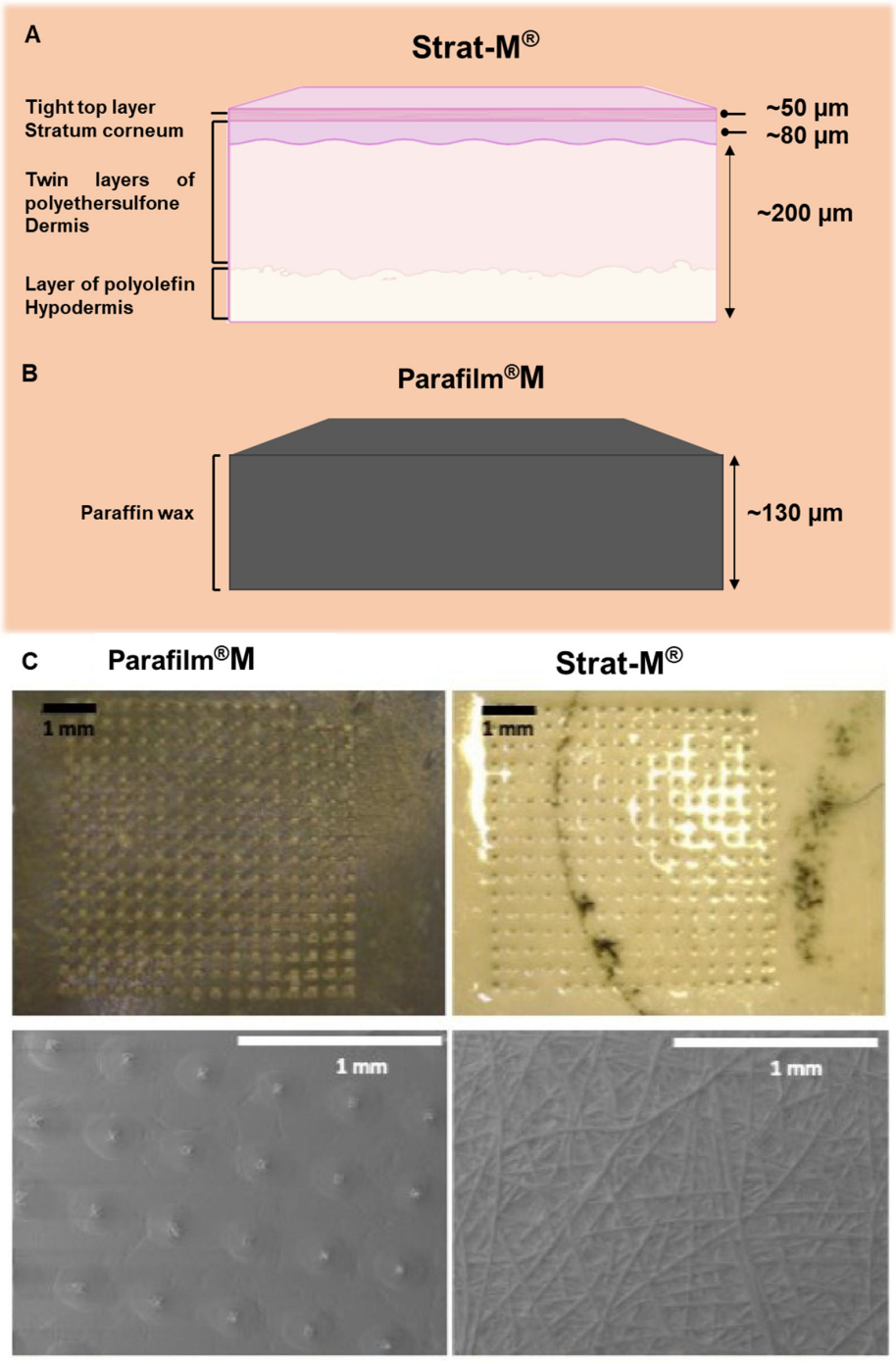


**Figure 2.** (**A**) Schematic illustration of the Strat-M® membrane, comprising a lipid-based top layer designed to approximate the barrier function of the stratum corneum, a porous polyethersulfone

middle layer providing dermis-like mechanical support, and a polyolefin non-fabric backing layer analogous to subcutaneous tissue. (**B**) Schematic illustration of the Parafilm®M tissue model, consisting of a single paraffin wax–based layer with a uniform thickness of approximately 130 µm. Panels (**A**,**B**) were redrawn with modifications from Ref. [19]. Some elements were created in BioRender. Kashaninejad (2026) https://BioRender.com/b4kk5wt/. (**C**) Representative experimental images showing microneedle penetration patterns in Parafilm®M and Strat-M® membranes: optical microscopy images of the membrane top surfaces (**upper row**) and corresponding SEM images of the membrane backside (**lower row**). Panel (**C**) is reproduced from Ref. [19] under the terms of the Creative Commons Attribution (CC BY 4.0) license.

Sometimes, the importance and accuracy of a particular aspect of MN performance necessitate the use of artificial tissue models alongside animal tissues. For example, in a recent study by Leite et al., the dissolution performance of single-component polysaccharide-based, lidocaine-loaded dissolving MNs (PL- Lid MNs) was evaluated using two different tissue models: agarose hydrogel and porcine ear skin [20]. The dissolution assay conducted on agarose gel showed results comparable to those on porcine skin tissue, with a similar dissolution rate and loss of integrity over the same time points. In both models, the microneedle tips were fully dissolved within 10 min of insertion. 26% and 32% of the lidocaine remained in the patch after insertion into agarose hydrogel and porcine skin, respectively.

#### 3.2.1. Cell–Laden Artificial Tissue Models

To evaluate cellular responses to therapeutic agents and assess treatment effectiveness, it is common to extend MN testing to cell-based platforms. To date, cytotoxicity analyses have primarily been conducted using 2D culture media. However, recent studies have begun to advance this approach by culturing cells within 3D tissue models, making the testing environment more complex and closely aligned with real physiological conditions.

It should be noted that while cell-laden artificial tissue models offer greater physiological relevance than acellular platforms, their broader adoption is often constrained by higher cost, increased experimental complexity, specialised infrastructure requirements, and limited scalability. As a result, advanced models such as 3D bioprinted tissues and skin-on-chip systems are predominantly used in academic and late-stage mechanistic studies, whereas simpler artificial tissue models remain more practical for routine screening, high-throughput testing, and industrial or translational workflows.

##### 3D Bioprinted Models

The antitumor activity of the dissolvable carboxymethylcellulose–fucoidan (CMC_Fuc) MNs against melanoma cells (A375 cell line) was evaluated using a 3D bioprinted cell-laden culture model (Figure 3A) [21]. The 3D in vitro model was fabricated using a bioink composed of a pectin nanocomposite hydrogel containing 4.7% ($w/v$) pectin, 2.0% ($w/v$) nanofibrillated cellulose (NFC), and 0.75% ($w/v$) lysozyme nanofibrils (LNFs), loaded with A375 cells at a density of $3 \times 10^6$ cells $mL^{-1}$. Using this structure offers several advantages, as it better mimics the natural physiological conditions of the tumor microenvironment, including cell–cell interactions, spatial complexity, and cellular communication, which are not adequately represented in conventional 2D cultures. The antitumor activity of the MNs was assessed in both 2D cell culture media and the 3D bioprinted cell-laden tissue model. The MN array exhibited a clear cytotoxic effect on A375 cells after 24 and 48 h of application in both culture systems, as reflected by the observed reduction in cell viability. In the 2D culture, cell viability decreased to 59 ± 4% after 24 h and 17 ± 7% after 48 h. In the 3D tissue model, viability was reduced to 68 ± 9% after 24 h and 44 ± 4% after 48 h. The comparatively stronger cytotoxic response in the 2D model is attributed to its lower physiological complexity relative to the 3D environment, which reduces cellular resistance to treatment and thereby increases susceptibility to the MN-induced antitumor effect.

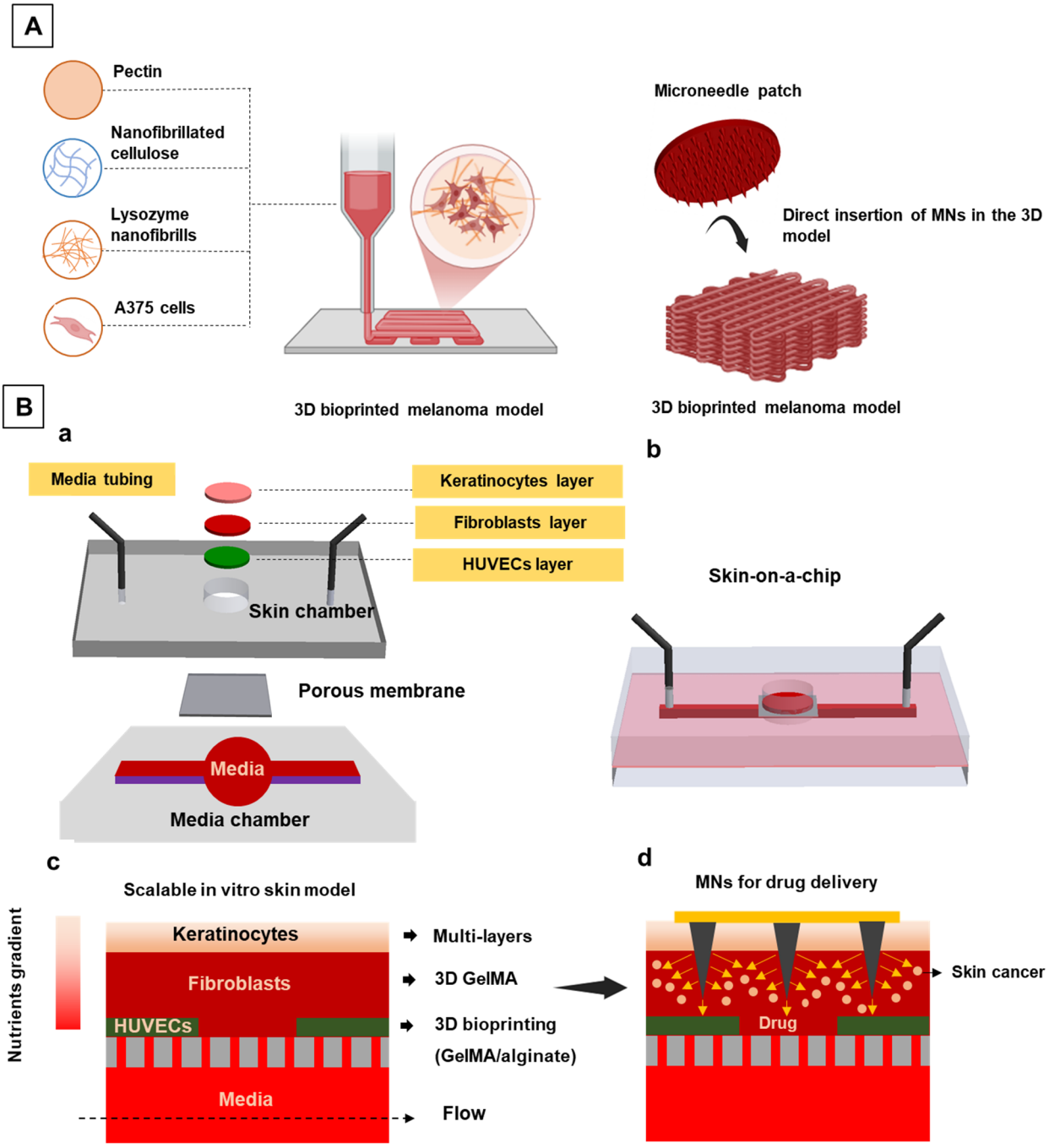


**Figure 3.** (**A**) Schematic illustration of the preparation mechanism of the bioprinted melanoma tissue model. Redrawn with some changes from [21]. Some elements were created in BioRender. Kashaninejad (2026) https://BioRender.com/2pnzpr0. (**B**) (**a**) Schematic of the skin-on-a-chip setup for MN analysis. (**b**) Scheme of the 3D assembled skin-on-a-chip model (**c**) Schematic illustration of the cross-sectional view of the skin-on-chip platform. (**d**) Schematic representation of MN-mediated drug delivery targeting melanoma cancer cells in a skin-on-a-chip melanoma model. Redrawn with some changes from [22].

## Wound Models

Another key concern with artificial skin models is their ability to replicate pathological or damaged tissue conditions. Addressing this issue, Silve et al. developed a reproducible wound model using a 3D skin construct [22]. The system consisted of a fully differentiated, stratified squamous epithelium derived from human keratinocytes grown at an air–liquid interface on a type I collagen scaffold seeded with human dermal fibroblasts. Wound

conditions were simulated using a microneedle stamping method, allowing the creation of length-tailored wound areas for therapeutic evaluation. The morphology, cell viability, and immunological responses at the simulated wound site were evaluated using histological staining, metabolic assays, and cytokine expression analysis.

Skin-on-a-Chip Platforms

Skin-on-a-chip platforms have been introduced as robust model systems that provide physiologically relevant conditions for disease modeling and drug efficacy analysis [23,24]. To investigate the progression of skin-related diseases and evaluate the effectiveness of drug treatments, a skin-on-a-chip model was developed by Barros et al. [23]. The system was designed on a PDMS-based microfluidic platform consisting of a microchannel for media perfusion, a porous polyester membrane (0.4 μm pore size), and a PDMS skin chamber, as shown in Figure 3B. The engineered skin model incorporated vascular layer, dermis and epidermis presenting enhanced functionality and maturation. Dermal layer development was confirmed by Collagen I and Fibronectin expression (after 7 days), while epidermal layer maturation was validated by the expression of Filaggrin and Keratin 10, 14, and 19 at the air–liquid interface (ALI) over 21 days. To simulate melanoma invasion into the dermis, melanoma cells were placed 400 μm below the epidermal layer, adjacent to the dermis. The skin-on-a-chip platform was subsequently utilized to assess the therapeutic efficacy of doxorubicin (DOX)-loaded gelatin methacryloyl (GelMA) MNs for targeted treatment of melanoma cancer cells.

### *3.3. Biosensing*

As for another application regarding the MN system, MNs present potential as biosensory system. The detection platform used in this system can be based on two main principles of on-site and off-site mechanisms. As with drug delivery performance analysis, the biosensing function of the MN array system should be monitored to ensure consistent results. The use of artificial tissue models for the preliminary steps of in vitro test series for microneedle performance assessment could serve as a reference for sensing function analysis. Employing artificial tissue samples allows the option of sensitivity analysis of the MN testing system under different conditions for a variety of biomarkers. Analyzing extreme conditions and manipulating the sensing environment are among the options offered through using these tissue-like platforms.

From a testing perspective, key biosensing performance metrics include sampling efficiency (extracted volume or uptake), analytical sensitivity and detection limit, response time, selectivity against interfering species, and signal stability in physiologically relevant media. Artificial tissue phantoms enable controlled modulation of analyte concentration and matrix composition (e.g., Phosphate-Buffered Saline (PBS) vs. interstitial fluid (ISF)), supporting reproducible benchmarking across these metrics.

A patch of porous microneedles containing glucose oxidase (GOx) and horseradish peroxidase (HRP), and a colorimetric sensing layer containing 3, 30, 5, 50-tetramethylbenzidine (TMB) on the back of the MNs was prepared for rapid glucose sampling and sensing [25]. For testing and validating the MN's performance in rapid fluid sampling and collection, an agarose gel was used as a tissue model containing simulated fluid. The volume of the fluid extracted from agarose gel was measured in different time intervals. $34.57 \pm 4.76$ mg of the loaded fluid in agarose gel was extracted in 1 min of patch wearing. Effects of different glucose concentrations on the performance of microneedles was also analyzed. A linear relationship was observed between the glucose content into the tissue structure and the recovered liquid volume by porous microneedles.

Manssouri Majd reported the preparation of a hydrogel-coated stainless-steel MN biosensor capable of selective and low-potential electrochemical glucose detection directly in skin-mimicking phantom [26]. For in vitro testing of electrochemical functionality, a phantom-gel tissue was modeled to simulate the mechanical and diffusional properties of human tissue. Two different phantom gels were formulated using either PBS or ISF to replicate the transdermal condition. Defined glucose concentrations, ranging from low (normal) to high (pathological) levels, were injected into the tissue models, and the electrochemical biosensing performance of the microneedles was evaluated under both conditions. The results demonstrated that both tissue models provided a promising skin-mimicking platform. However, the microneedle biosensor exhibited higher sensitivity in PBS than in ISF, attributed to the presence of multivalent ions and organic constituents in ISF that may interfere with detection. The biosensor's selectivity, an essential feature given that microneedles operate in a complex microenvironment, was further evaluated by introducing interfering analytes, such as ascorbic acid, uric acid, and acetaminophen, at physiological or supraphysiological levels.

The analytical performance of a wearable MN sensor for cholesterol monitoring was evaluated using an artificial skin phantom [27]. The device consisted of pyramidal microneedles with hollow side microcavities integrated with platinum (Pt) and silver (Ag) wires. Cholesterol oxidase (ChOx) was immobilized on the Pt transducer surface using bovine serum albumin and Nafion. The microcavity design protected the immobilized enzyme layer during MN insertion into the tissue.

To avoid the effects of long-term exposure to complex biological media on sensor performance, the analysis was conducted using artificial media, including ISF and a skin-mimicking gel phantom. A 1.4% agarose gel prepared by dissolving agarose powder in PBS was used as the artificial tissue platform. Five different cholesterol concentrations (2–10 μM) were tested by diffusing cholesterol into the gel, after which the MNs were inserted and left in place for 1 min to ensure contact between the MN tips and the tissue. Cholesterol levels were quantified by amperometric measurements. The resulting calibration curve between current and cholesterol concentration, obtained from chronoamperometric responses, exhibited a linear dynamic range across the tested concentrations, with a correlation coefficient of 0.9996, demonstrating the potential of the biosensor for cholesterol monitoring. In addition, the selectivity of the sensor was confirmed in the presence of potential interfering species, including glucose, lactic acid, uric acid, and ascorbic acid, together with cholesterol.

A summary of the reported studies is presented in Table 1.

The use of artificial tissue models for microneedle characterization provides valuable insights into multiple aspects of microneedle performance. As highlighted in the existing literature, these models can be tailored to replicate conditions most relevant to specific applications. In this context, artificial tissues can be regarded as purpose-designed, engineered testing platforms. For example, in hydrogel-based tissues such as agarose gels, the mechanical properties can be tuned by adjusting the agarose concentration to match those of the target tissue. Similarly, while simple gel-based structures are sufficient for mechanical testing, they are not suitable for evaluating drug therapeutic efficacy; in such cases, cell-laden tissue models provide a more appropriate platform. Based on these considerations, a decision framework for selecting artificial tissue models based on application and performance metrics is presented in Table 2.

Collectively, these studies show that artificial tissue models are particularly valuable for early-stage calibration and selectivity testing, but they remain limited in replicating dynamic physiological exchange (e.g., ISF replenishment and immune-related fouling), reinforcing the need for hybrid or perfused platforms in later-stage validation.

**Table 1.** Summary of the reported studies employing artificial tissue models for various applications.

| MN Design | MN Application | Tissue Type | Key Findings |
| --- | --- | --- | --- |
| 3D-printed solid MNs [14] | Tissue adhesion | 2% agarose gel | The mechanical insertion and extraction behavior of the needles was analyzed using an agarose tissue model that simulates human tissues. |
| Hydrogel MNs [15] | Penetration study | A composite tissue model composed of a silicone layer and a gel layer | The tissue model demonstrated greater physiological relevance to biological tissues in terms of microneedle penetration depth, drug permeation, and heating profile compared to the agarose model |
| PVP/PVA dissolving MNs for cubosome-like rapamycin-loaded nanoparticles [18] | Drug delivery | 3% agarose gel | The transparency of agarose gel makes it an excellent model for visualizing drug diffusion pathways. |
| Dissolving microneedle patch for protein (ovalbumin, bovine serum albumin and amniotic mesenchymal stem cell metabolite products) transdermal delivery [19] | Transdermal protein delivery | Parafilm®M, and Strat-M® | Synthetic membranes were able to bypass protein-related skin interference in in vitro permeation studies, thereby providing more reliable results. |
| Polysaccharide-based, lidocaine-loaded dissolving microneedles (PL- Lid MNs) [20] | Drug delivery | Agarose with a layer of Parafilm. | The microneedle dissolution rate in agarose hydrogel was found to be comparable to that in porcine ear skin. |
| Carboxymethylcellulose-fucoidan dissolvable MN [21] | Drug delivery, anti tumoral analysis | 3D bioprinted melanoma culture mode | The bioprinted tissue mimics the natural physiological conditions of the tumor microenvironment, including cell–cell interactions, spatial complexity, and cellular communication |
| A stamp with incorporated needles with a length of 250 µm [22] | Wound modeling | Artificial 3D human skin simulated tissue model | Length-tailored wounds were simulated in a 3D skin model to study cell migration and interactions during the wound healing process, as well as to better understand tissue regeneration in response to various factors. |
| Doxorubicin (DOX)-loaded gelatin methacryloyl (GelMA) MNs [23] | Transdermal drug delivery | Skin-on-a-chip platform | Skin-on-a-chip platform was utilized to assess the therapeutic efficacy of doxorubicin (DOX)-loaded gelatin methacryloyl (GelMA) MNs for targeted treatment of melanoma cancer cells. |
| A patch of porous microneedles containing glucose oxidase (GOx) and horseradish peroxidase (HRP), and a colorimetric sensing layer (TMB) on the back of the microneedles [25] | Glucose sensing | Agarose gel | The performance of microneedles was evaluated across a spectrum of glucose concentrations, ranging from normal to abnormal levels. |
| Hydrogel-coated stainless-steel microneedle biosensor [26] | Selective and low-potential electrochemical glucose detection | Agarose gel | The sensitivity of the microneedle patch was evaluated using two different phantom gels formulated with PBS or ISF. Selectivity was assessed in the presence of potential interfering substances. |
| Biocatalytic MN wearable sensor [27] | Cholesterol monitoring | Agarose gel | The potential of the MNs for continuous cholesterol monitoring in ISF was demonstrated, together with an evaluation of its selectivity in the presence of potential interfering species. |

**Table 2.** Decision framework for selecting artificial tissue models based on application, performance metrics, validation requirements, and practical constraints.

| Use Case | Performance Metric | Required Tissue Properties | Recommended Artificial Models |
|---|---|---|---|
| MN insertion testing | Insertion/extraction force/ MN penetrability | Elastic modulus/viscoelasticity | Composite gel, agarose gel, silicone elastomer, Parafilm |
| Drug release performance | Drug diffusion pathway, MN dissolution rate | Diffusivity, porosity, hydration, optical transparency | Agarose gel |
| Drug therapeutic effect | Cell–cell interaction, drug response analysis | Cell integrated | Skin-on-a-chip platform/ cell integrated 3D printed tissue model |
| Biosensing | Sensitive and selective biomarker selection | Fluid availability, interference transport, biomarker transport | Agarose gel |

## 4. Limitations and Challenges

Despite the significant advantages of artificial tissue models for MN testing and post-analysis, several challenges persist. These models cannot fully replicate the structural, mechanical, and functional characteristics of real biological tissues, as summarized schematically in Figure 4. The unique morphology of each tissue type plays a crucial role in microneedle penetration and overall performance, which may not be accurately simulated in artificial platforms.

It should be noted that the merits and limitations summarised in Figure 4 primarily reflect skin-mimicking artificial tissue models, which constitute the majority of currently reported platforms for MN testing. Artificial tissue phantoms developed for non-transdermal targets are comparatively scarce, remain highly application-specific, and are still at an early stage of development; therefore, they are beyond the primary scope of the present schematic comparison.

For instance, the curvature and delicate structure of ocular tissue pose specific challenges for artificial reproduction of ocular MN applications. In addition, physiological responses, such as tearing induced by the sustained absence of blinking, cannot be mimicked in vitro. Similarly, if the target tissue is the breast, natural movements associated with respiration (e.g., chest expansion and relaxation) introduce dynamic mechanical conditions that are not easily simulated in artificial environments.

Another major limitation is the absence of systemic physiological components. Artificial tissue models lack integration with blood circulation, immune responses, and drug clearance pathways, all of which play critical roles in drug delivery and therapeutic outcomes. Likewise, for fluid extraction applications, replicating the dynamics of ISF flow remains a significant challenge.

Emerging hybrid platforms, such as perfused microfluidic or organ-on-chip systems that integrate artificial tissue constructs with controlled flow and, in some cases, endothelial or immune cell components, represent a promising research direction for addressing these dynamic physiological limitations; however, their application to microneedle testing remains largely exploratory and is currently limited by scalability, cost, and experimental complexity.

It can be confidently stated that artificial tissue platforms are essential for in vitro microneedle testing and analysis during the early stages of MN development. Given the high costs of microneedle design and fabrication, these models offer a practical, cost-effective approach to overcoming challenges associated with repeated testing and design

iteration. However, despite their advantages, artificial tissue platforms may still have limitations when used in the final stages of microneedle evaluation test series.

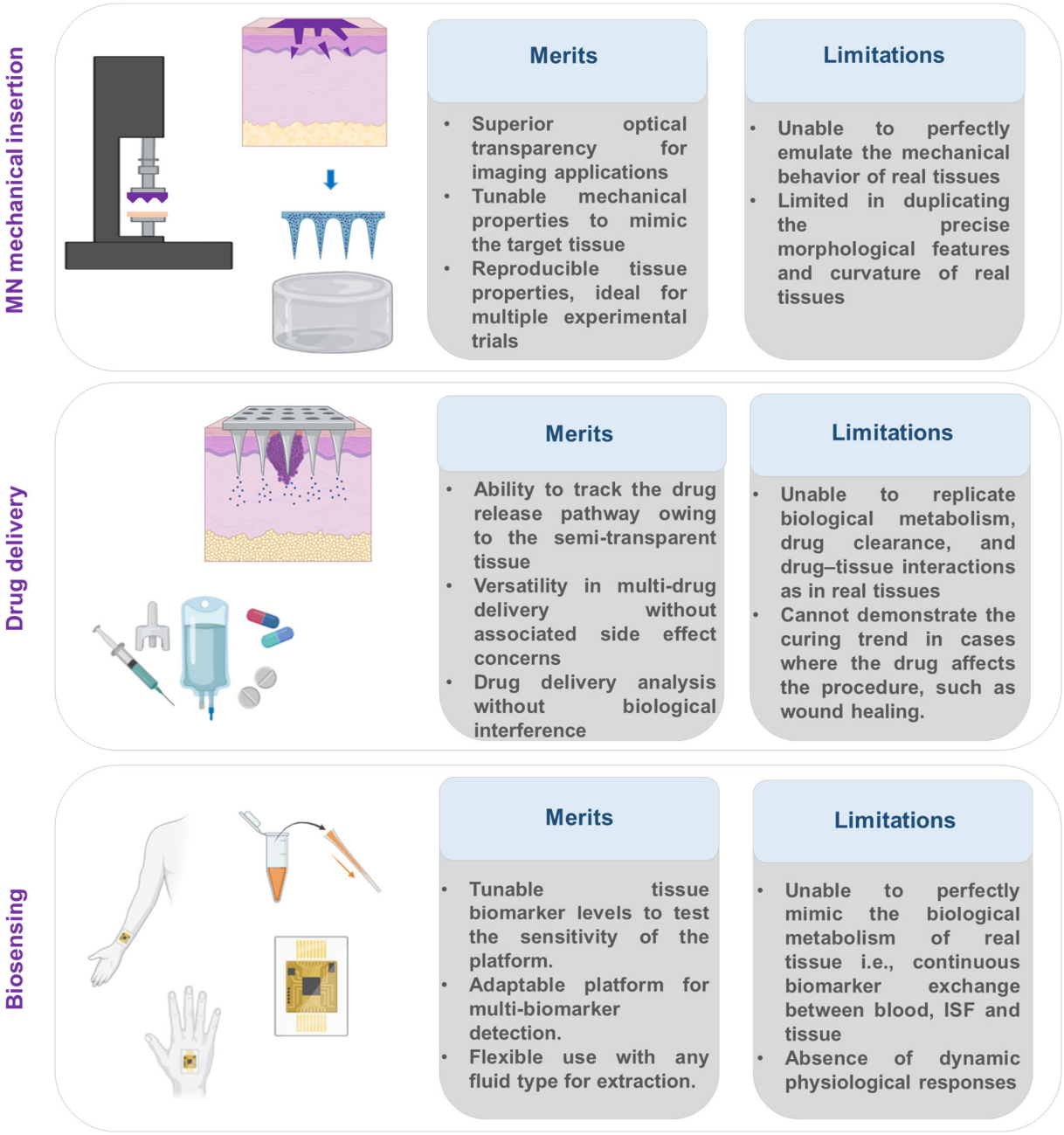


**Figure 4.** Key information on the merits and limitations of artificial tissue models in microneedle studies. Elements were Created in BioRender. Kashaninejad (2026) https://BioRender.com/gyzphcb.

## 5. Commercial Readiness of Artificial Tissue Platforms

Looking ahead, and with heightened awareness following recent global health crises, MN-based medical technologies are poised to play an increasingly important role in healthcare delivery. As standardized testing workflows and safe production pathways become increasingly critical, robust, reliable characterization platforms have become a high priority. Consequently, there is a clear and growing need to advance the commercialization of artificial tissue models as realistic tissue surrogates, in parallel with the rapid technological progress of MN systems.

A useful framework for describing and benchmarking the maturity of such emerging characterization platforms is the Technology Readiness Level (TRL) scale, originally developed by the National Aeronautics and Space Administration (NASA) and now widely adopted across engineering, biomedical, and translational research domains. TRL defines technology maturation across 9 levels, ranging from fundamental concept formulation (TRL 1) to fully deployed, commercially operational systems (TRL 9) [28]. Within translational research, this framework has proven particularly valuable for identifying gaps between laboratory proof-of-concept and practical deployment—commonly referred to as the "valley of death" [29].

In the context of artificial tissue models for MN evaluation, most reported platforms currently reside in the mid-TRL range (approximately TRL 3–5), where feasibility has been demonstrated through laboratory validation and controlled testing.

At present, several commercially available artificial tissue surrogates are already used within MN research and development workflows. For example, Strat-M®, a multilayer synthetic membrane designed to approximate key barrier properties of human skin, is widely employed for in vitro drug permeation and release studies involving MN-mediated delivery. Similarly, Parafilm®M and standardized polymeric or hydrogel substrates are frequently used as reproducible benchmarks for MN insertion, penetration depth, and mechanical integrity testing. These platforms offer clear advantages in terms of accessibility, reproducibility, and ease of integration into early-stage screening and comparative testing protocols.

Accordingly, simple artificial tissue models are more commonly adopted in industrial and translational settings, where throughput, reproducibility, and cost-efficiency are prioritised, whereas advanced tissue-engineered platforms remain largely confined to academic laboratories due to scalability and cost constraints.

From a validation perspective, progression toward higher TRL requires the establishment of clear and repeatable performance benchmarks. These include demonstration of repeatability and reproducibility through batch-to-batch consistency and, where feasible, inter-laboratory validation, as well as benchmarking against relevant ex vivo or in vivo tissues using matched performance metrics (e.g., insertion force, penetration depth, permeation rate, or analyte recovery). For commercial deployment, additional practical considerations include quality-control (QC) procedures, material consistency, shelf stability under defined storage conditions, and compatibility with standardized testing workflows. Together, these steps represent concrete milestones for advancing artificial tissue platforms from research tools toward robust, commercially viable testing standards.

Despite their commercial availability, the broader adoption of such platforms at higher TRLs remains limited. One major barrier is their inability to replicate critical aspects of biological complexity relevant to late-stage validation, including tissue heterogeneity, vascularization, immune response, active metabolism, and long-term drug distribution. In addition, many commercially available artificial tissues are application-specific, meaning that performance metrics obtained using a given platform may not be directly transferable across different MN designs, payloads, or target tissues. The absence of formal regulatory qualification pathways and limited inter-laboratory benchmarking further constrain their acceptance as standalone validation tools for advanced development stages.

It is also essential to recognise that TRL, while widely used, is not without limitations. Studies examining TRL implementation across multiple industries have highlighted challenges related to assessment validity, system complexity, and contextual interpretation, particularly as technologies approach higher readiness levels [28]. These findings emphasise that TRL alone cannot fully capture integration requirements, workflow compatibility, or the robustness of validation protocols, all of which are critical for commercial deploy-

ment. Consequently, the practical application of TRL frameworks in translational contexts often requires adaptation to sector-specific constraints and the provision of supporting evidence beyond nominal readiness classification.

For artificial tissue surrogates, this suggests that advancement toward commercial readiness will depend on demonstrating consistent performance across multiple microneedle designs, compatibility with industry-standard testing workflows, and documentation practices aligned with recognised quality and safety frameworks, such as those established by the International Organization for Standardization (ISO) and the Food and Drug Administration (FDA).

Ultimately, commercially available artificial tissue platforms are best positioned as standardized preclinical screening and benchmarking tools, rather than replacements for ex vivo or in vivo testing. Continued development toward higher TRLs has the potential to accelerate MN development, reduce development risk, and enable faster and safer market entry for MN-based technologies.

## 6. Conclusions and Future Perspective

With the rapid advancement in microneedle research, the need for a reliable, scalable characterization platform has become increasingly evident. From penetration to application (e.g., therapy or sensing), microneedle functionality must be rigorously evaluated with respect to insertion mechanics, drug delivery efficiency, and biosensing capabilities. Given the need for multiple characterization tests, artificial tissue platforms that closely simulate the properties of real tissues offer an excellent alternative for microneedle performance assessment, as they circumvent several challenges associated with in vivo and ex vivo tissue models.

This paper aimed to provide a distinct perspective on these artificial surrogates, which have consistently complemented in vivo tests during the microneedle evaluation process. It should be noted that, despite their flexibility and demonstrated potential as tissue mimics, the use of artificial models has thus far been largely restricted to the early stages of microneedle development and has not yet found widespread adoption in final evaluation stages. This limitation is likely due to their inability to fully replicate the complexity of real tissues.

Such dissimilarity, however, can be considered a double-edged sword. On one hand, simplified models are advantageous for preliminary testing, as they allow researchers to isolate and investigate specific aspects of microneedle functionality without interference. On the other hand, the absence of these biological interferences, which are an inseparable part of real tissues, can sometimes lead to findings that diverge from in vivo performance.

Looking forward, bridging this gap between early-stage screening and advanced evaluation will be critical not only for improving physiological relevance but also for enabling broader adoption of artificial tissue platforms in translational and industrial settings. In this context, continued development of standardized, scalable, and application-relevant artificial tissue models will be essential to support the reliable advancement of microneedle technologies toward clinical use and commercial deployment. Future progress is likely to benefit from the co-design of MN devices and artificial tissues, in which phantom specifications are iteratively refined alongside microneedle geometry, materials, and intended function.

To enable translation and cross-laboratory comparability, standardized benchmarks for artificial tissues should be defined in terms of measurable mechanical, transport, and reproducibility metrics. We propose a three-tier framework: (i) mechanical benchmarks, including elastic modulus, fracture stress, and toughness, which govern microneedle insertion physics; (ii) transport benchmarks, including water content, porosity, diffusion

coefficient, and permeability, which control drug delivery and biosensing performance; and (iii) reproducibility benchmarks, such as batch-to-batch variation in the modulus, insertion force, and analyte uptake, with acceptable coefficients of variation below 10–15%. Artificial tissues meeting these criteria can serve as standardized, application-specific reference platforms for microneedle evaluation.

It is worthwhile to direct greater efforts in research and development toward creating more realistic artificial samples for advanced microneedle evaluation. For instance, three-dimensional bioprinting technologies capable of generating functional tissue-like architectures represent a promising approach in this direction [30].

**Author Contributions:** Conceptualization, N.K. and E.L.Z.; Literature review and analysis, E.L.Z.; Writing—original draft preparation, E.L.Z.; Writing—review and editing, N.K. Visualization, E.L.Z.; Supervision, N.K. All authors have read and agreed to the published version of the manuscript.

**Funding:** This research was funded by the Australian Research Council (ARC) Discovery Early Career Research Award (DECRA) (DE220100205).

**Informed Consent Statement:** Not applicable.

**Data Availability Statement:** Data sharing is not applicable to this article.

**Acknowledgments:** The authors acknowledge the School of Engineering and Built Environment (EBE) at Griffith University for providing a supportive research environment and institutional support during the preparation of this review.

**Conflicts of Interest:** The authors declare no conflicts of interest.

## References

1. Lori Zoudani, E.; Nguyen, N.T.; Kashaninejad, N. Microneedle optimization: Toward enhancing microneedle's functionality and breaking the traditions. *Small Struct.* **2024**, *5*, 2400121. [CrossRef]
2. Zhu, Z.; Wang, J.; Pei, X.; Chen, J.; Wei, X.; Liu, Y.; Xia, P.; Wan, Q.; Gu, Z.; He, Y. Blue-ringed octopus-inspired microneedle patch for robust tissue surface adhesion and active injection drug delivery. *Sci. Adv.* **2023**, *9*, eadh2213. [CrossRef]
3. Long, L.; Ji, D.; Hu, C.; Yang, L.; Tang, S.; Wang, Y. Microneedles for in situ tissue regeneration. *Mater. Today Bio* **2023**, *19*, 100579. [CrossRef]
4. Cheng, J.; Huang, J.; Xiang, Q.; Dong, H. Hollow microneedle microfluidic paper-based chip for biomolecules rapid sampling and detection in interstitial fluid. *Anal. Chim. Acta* **2023**, *1255*, 341101. [CrossRef]
5. Zhu, J.; Zhou, X.; Kim, H.J.; Qu, M.; Jiang, X.; Lee, K.; Ren, L.; Wu, Q.; Wang, C.; Zhu, X. Gelatin methacryloyl microneedle patches for minimally invasive extraction of skin interstitial fluid. *Small* **2020**, *16*, 1905910. [CrossRef]
6. Han, D.; Morde, R.S.; Mariani, S.; La Mattina, A.A.; Vignali, E.; Yang, C.; Barillaro, G.; Lee, H. 4D printing of a bioinspired microneedle array with backward-facing barbs for enhanced tissue adhesion. *Adv. Funct. Mater.* **2020**, *30*, 1909197. [CrossRef]
7. Muresan, P.; McCrorie, P.; Smith, F.; Vasey, C.; Taresco, V.; Scurr, D.J.; Kern, S.; Smith, S.; Gershkovich, P.; Rahman, R. Development of nanoparticle loaded microneedles for drug delivery to a brain tumour resection site. *Eur. J. Pharm. Biopharm.* **2023**, *182*, 53–61. [CrossRef] [PubMed]
8. Detamornrat, U.; Parrilla, M.; Domínguez-Robles, J.; Anjani, Q.K.; Larrañeta, E.; De Wael, K.; Donnelly, R.F. Transdermal on-demand drug delivery based on an iontophoretic hollow microneedle array system. *Lab Chip* **2023**, *23*, 2304–2315. [CrossRef] [PubMed]
9. Barisam, M.; Saidi, M.S.; Kashaninejad, N.; Vadivelu, R.; Nguyen, N.-T. Numerical Simulation of the Behavior of Toroidal and Spheroidal Multicellular Aggregates in Microfluidic Devices with Microwell and U-Shaped Barrier. *Micromachines* **2017**, *8*, 358. [CrossRef]
10. Makvandi, P.; Kirkby, M.; Hutton, A.R.; Shabani, M.; Yiu, C.K.; Baghbantaraghdari, Z.; Jamaledin, R.; Carlotti, M.; Mazzolai, B.; Mattoli, V. Engineering microneedle patches for improved penetration: Analysis, skin models and factors affecting needle insertion. *Nano-Micro Lett.* **2021**, *13*, 93. [CrossRef] [PubMed]
11. Permana, A.D.; Mir, M.; Utomo, E.; Donnelly, R.F. Bacterially sensitive nanoparticle-based dissolving microneedles of doxycycline for enhanced treatment of bacterial biofilm skin infection: A proof of concept study. *Int. J. Pharm. X* **2020**, *2*, 100047. [CrossRef] [PubMed]

12. Alrimawi, B.H.; Lee, J.Y.; Ng, K.W.; Goh, C.F. In vitro evaluation of microneedle strength: A comparison of test configurations and experimental insights. *RSC Pharm.* **2024**, *1*, 227–233. [CrossRef]
13. Karunanithi, S.; Rajappan, K. Biofunctionalized agarose-based biopolymer composites for advanced biomedical applications: A review. *Polym. Bull.* **2025**, *82*, 4835–4877. [CrossRef]
14. Zoudani, E.L.; De Saram, P.; Engel, K.; Nguyen, N.-T.; Kashaninejad, N. Microneedle–Tissue Interaction Across Varying Biological and Mechanical Conditions. *Biosensors* **2025**, *15*, 521. [CrossRef] [PubMed]
15. Makvandi, P.; Shabani, M.; Rabiee, N.; Anjani, Q.K.; Maleki, A.; Zare, E.N.; Sabri, A.H.B.; De Pasquale, D.; Koskinopoulou, M.; Sharifi, E. Engineering and development of a tissue model for the evaluation of microneedle penetration ability, drug diffusion, photothermal activity, and ultrasound imaging: A promising surrogate to ex vivo and in vivo tissues. *Adv. Mater.* **2023**, *35*, 2210034. [CrossRef]
16. Amer, M.; Chen, R.K. Self-Adhesive microneedles with interlocking features for sustained ocular drug delivery. *Macromol. Biosci.* **2020**, *20*, 2000089. [CrossRef]
17. Razzaghi, M. Polymeric 3D-Printed Microneedle Arrays for Non-Transdermal Drug Delivery and Diagnostics. *Polymers* **2025**, *17*, 1982. [CrossRef]
18. Ramalheiro, A.; Paris, J.L.; Silva, B.F.; Pires, L.R. Rapidly dissolving microneedles for the delivery of cubosome-like liquid crystalline nanoparticles with sustained release of rapamycin. *Int. J. Pharm.* **2020**, *591*, 119942. [CrossRef]
19. Anjani, Q.K.; Nainggolan, A.D.C.; Li, H.; Miatmoko, A.; Larrañeta, E.; Donnelly, R.F. Parafilm®M and Strat-M® as skin simulants in in vitro permeation of dissolving microarray patches loaded with proteins. *Int. J. Pharm.* **2024**, *655*, 124071. [CrossRef]
20. Leite, J.M.; Silva, A.C.; Jesus, A.; da Cruz, B.C.; Vieira, S.I.; Dias-Pereira, P.; Costa, P.C.; Almeida, I.F.; Correia-Sá, I.; Silvestre, A.J. Single Polysaccharide Dissolvable Microneedles for Painless Local Anesthesia: Fabrication, Characterization, and In Vitro Neuronal Imaging. *ACS Biomater. Sci. Eng.* **2025**, *11*, 5426–5439. [CrossRef]
21. Silva, A.C.; Teixeira, M.C.; Jesus, A.; Costa, P.C.; Almeida, I.F.; Dias-Pereira, P.; Correia-Sá, I.; Oliveira, H.; Silvestre, A.J.; Vilela, C. Carboxymethylcellulose-fucoidan dissolvable microneedle patches for minimally invasive melanoma treatment: Demonstration on a 3D bioprinted A375 cell line model. *Int. J. Biol. Macromol.* **2025**, *319*, 145320. [CrossRef]
22. Salazar Silva, C.S.; Petzold, W.; Hirsch, U.; Schmelzer, C.E.; Friedmann, A. A standardized in vitro bioengineered skin for penetrating wound modeling. *Vitr. Models* **2025**, *4*, 15–30. [CrossRef]
23. Barros, N.R.; Kang, R.; Kim, J.; Ermis, M.; Kim, H.-J.; Dokmeci, M.R.; Lee, J. A human skin-on-a-chip platform for microneedling-driven skin cancer treatment. *Mater. Today Bio* **2025**, *30*, 101399. [CrossRef]
24. Chaturvedi, D.; Gore, M.; Yadav, S.; Majumder, A.; Jain, R.; Dandekar, P. A 3D microfluidic model for preclinical drug permeation studies: Advancing validation of skin-on-chip technology. *J. Pharm. Biomed. Anal.* **2025**, *268*, 117187. [CrossRef]
25. Zeng, Q.; Xu, M.; Hu, W.; Cao, W.; Zhan, Y.; Zhang, Y.; Wang, Q.; Ma, T. Porous colorimetric microneedles for minimally invasive rapid glucose sampling and sensing in skin interstitial fluid. *Biosensors* **2023**, *13*, 537. [CrossRef]
26. Majd, S.M. Hydrogel-coated microneedle biosensor for selective and low-potential glucose detection in skin-mimicking interstitial fluid phantoms. *Talanta* **2026**, *297*, 128555. [CrossRef]
27. Li, Z.; Kadian, S.; Mishra, R.K.; Huang, T.; Zhou, C.; Liu, S.; Wang, Z.; Narayan, R.; Zhu, Z. Electrochemical detection of cholesterol in human biofluid using microneedle sensor. *J. Mater. Chem. B* **2023**, *11*, 6075–6081. [CrossRef]
28. Olechowski, A.L.; Eppinger, S.D.; Joglekar, N.; Tomaschek, K. Technology readiness levels: Shortcomings and improvement opportunities. *Syst. Eng.* **2020**, *23*, 395–408. [CrossRef]
29. Bhattacharya, S.; Kumar, V.; Nishad, S.N. Technology Readiness Level: An Assessment of the Usefulness of this Scale for Translational Research. *Productivity* **2022**, *62*, 112–124. [CrossRef]
30. Yadav, S.; Nguyen, N.-T. Three-dimensional models of human skin for biomedical applications. *Biophys. Rev.* **2025**, *6*, 031303. [CrossRef]